Granulocyte-derived Resistin Inhibits Monocyte Maturation and Promotes an Immunosuppressive Phenotype in Chronic Myelomonocytic Leukemia Monocytes

Supplemental tables:

Supplemental Table 1: Patient information (Discovery cohort)

Supplemental Table 2: Genes upregulated or downregulated in CMML granulocytes compared to all granulocytes

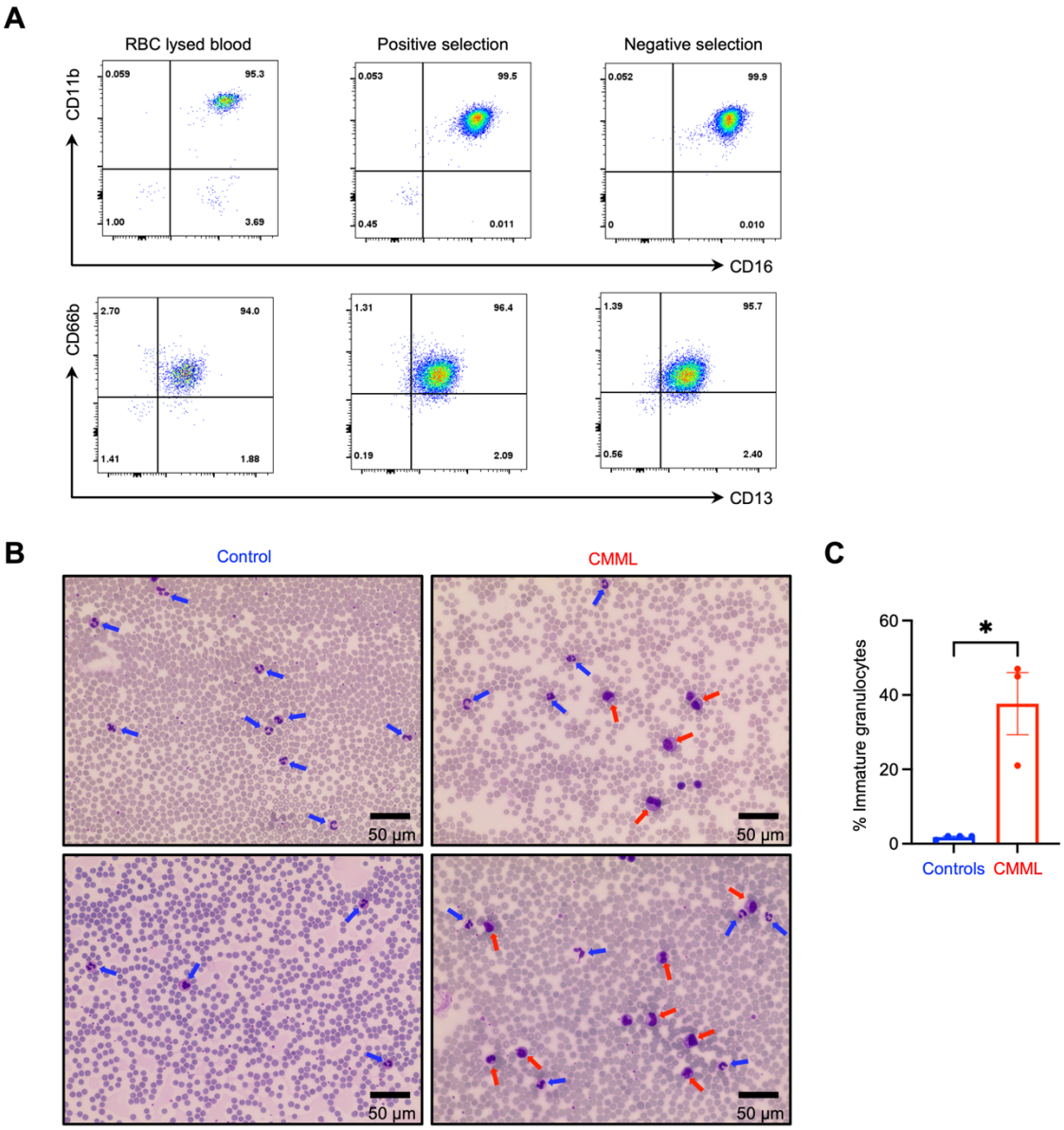
Supplemental Table 3: Multivariable analysis (Discovery cohort)

Supplemental Table 4: Patient information (Validation cohort)

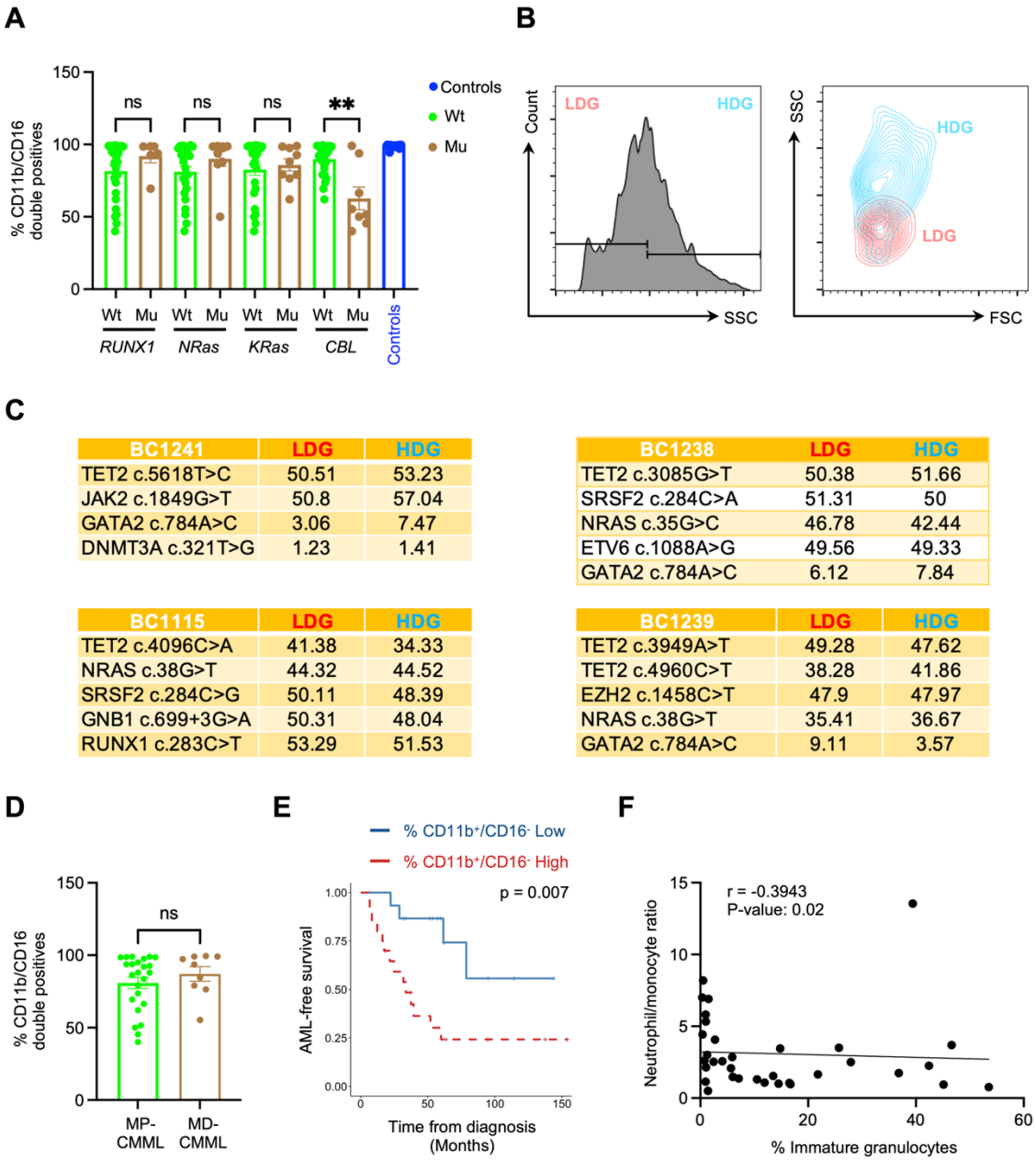
Supplemental Table 5: Multivariable analysis (validation cohort)

Supplemental Table 6: Genes upregulated or down regulated in healthy monocytes treated with resistin for 6 hrs in comparison with GFP control.

Supplemental Table 7: Genes upregulated or downregulated in healthy monocytes treated with resistin for 24 hrs in comparison with GFP control.



Supplemental Figure 1: (**A**) Representative flow cytometry plots displaying the expression of granulocytic markers CD11b, CD16, CD13, and CD66b on gated granulocytes (based on SSC) from RBC lysed fresh blood or granulocytes isolated using positive or negative selection methods. (**B**) Representative images showing the peripheral blood changes in granulocytes from age-matched healthy controls and CMML patients. Blue arrow points to mature granulocytes and red arrow points to immature granulocytes. (**C**) Bar graph depicting percentage of immature granulocytes found in healthy (n = 4) and CMML (n = 3) peripheral blood smear slides. Scale bar: 50 µm. Error bars = ± SEM; Mann-Whitney test; *, P<0.05.



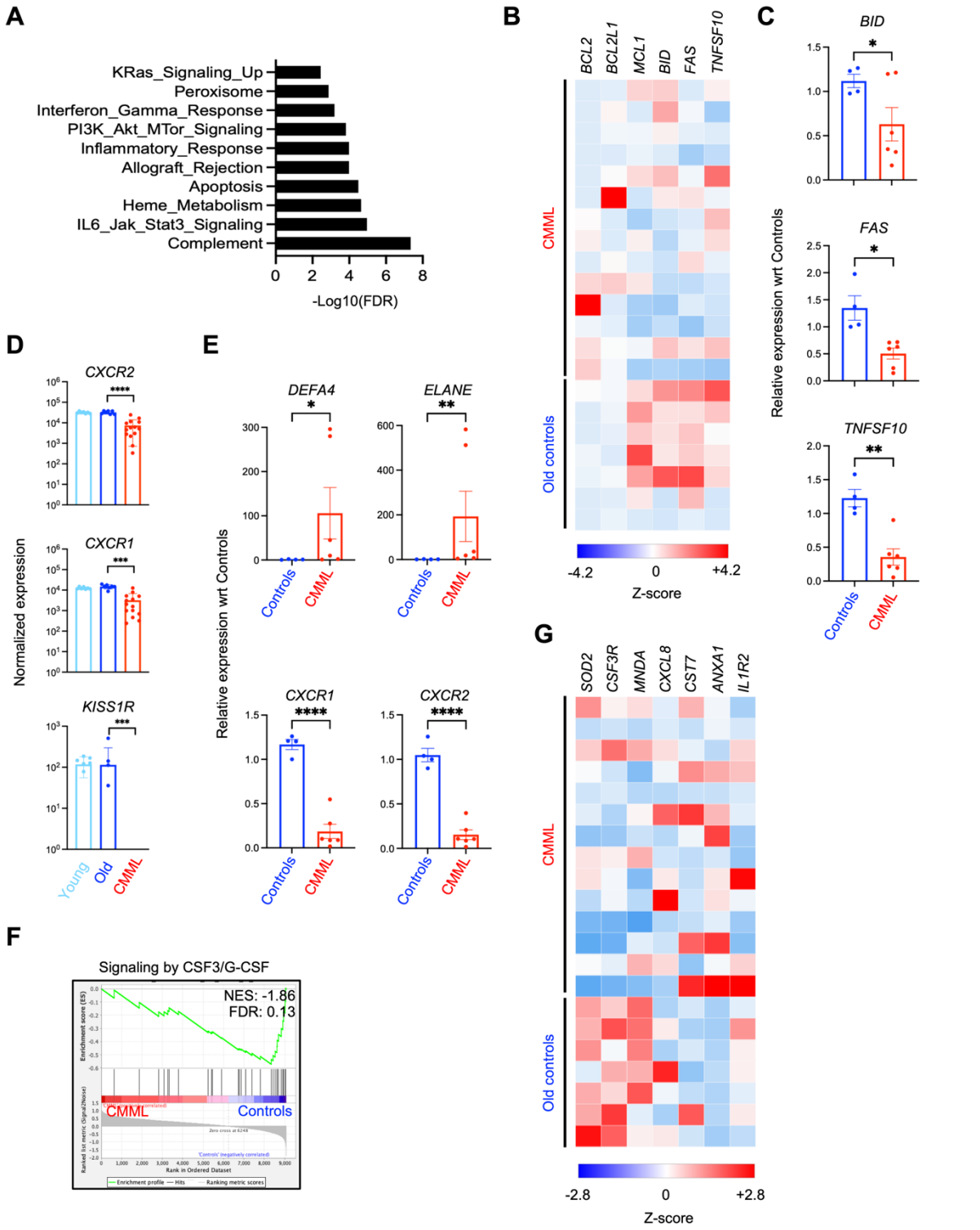
BC1241	LDG	HDG
TET2 c.5618T>C	50.51	53.23
JAK2 c.1849G>T	50.8	57.04
GATA2 c.784A>C	3.06	7.47
DNMT3A c.321T>G	1.23	1.41

BC1238	LDG	HDG
TET2 c.3085G>T	50.38	51.66
SRSF2 c.284C>A	51.31	50
NRAS c.35G>C	46.78	42.44
ETV6 c.1088A>G	49.56	49.33
GATA2 c.784A>C	6.12	7.84

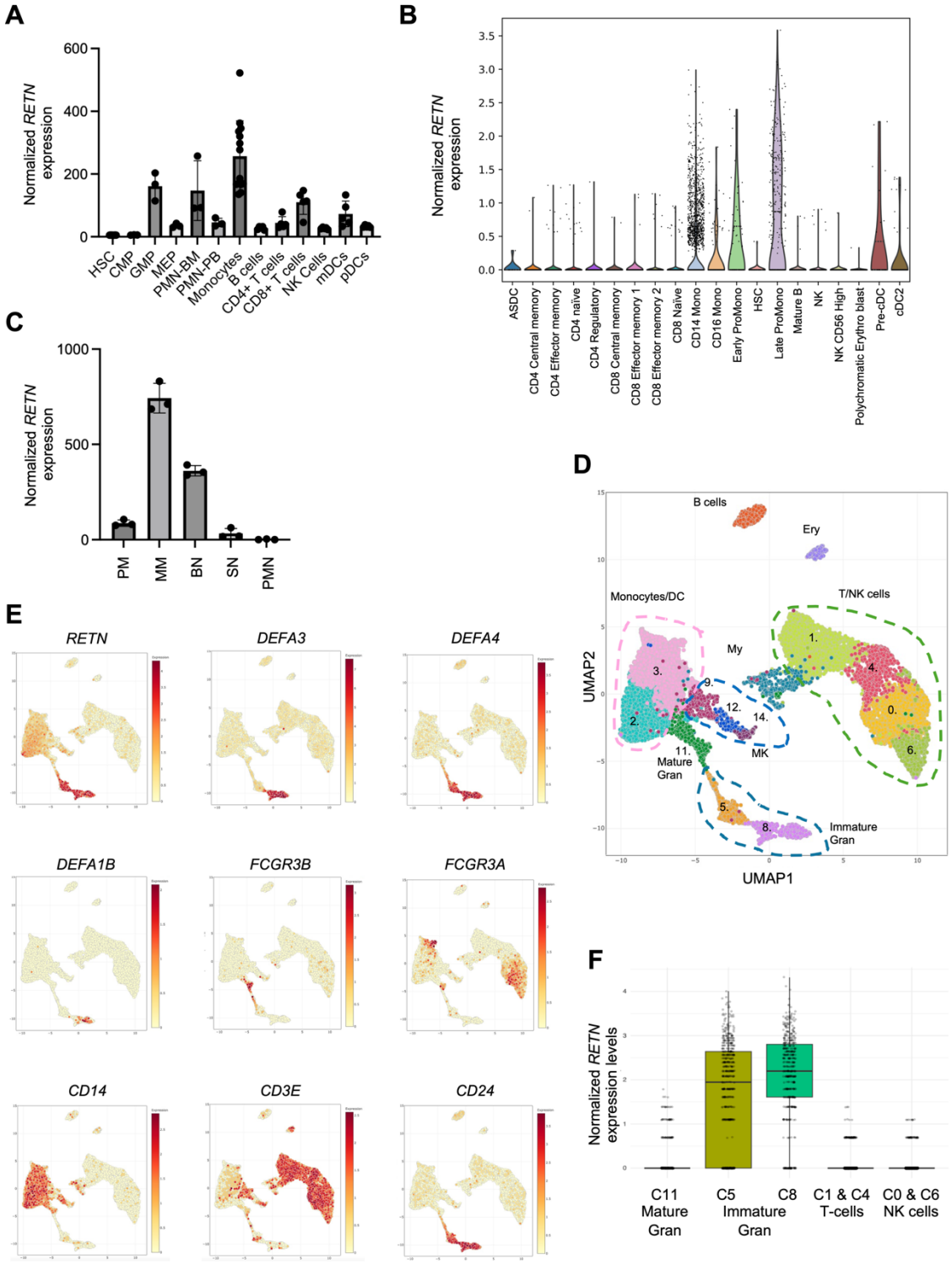
BC1115	LDG	HDG
TET2 c.4096C>A	41.38	34.33
NRAS c.38G>T	44.32	44.52
SRSF2 c.284C>G	50.11	48.39
GNB1 c.699+3G>A	50.31	48.04
RUNX1 c.283C>T	53.29	51.53

BC1239	LDG	HDG
TET2 c.3949A>T	49.28	47.62
TET2 c.4960C>T	38.28	41.86
EZH2 c.1458C>T	47.9	47.97
NRAS c.38G>T	35.41	36.67
GATA2 c.784A>C	9.11	3.57

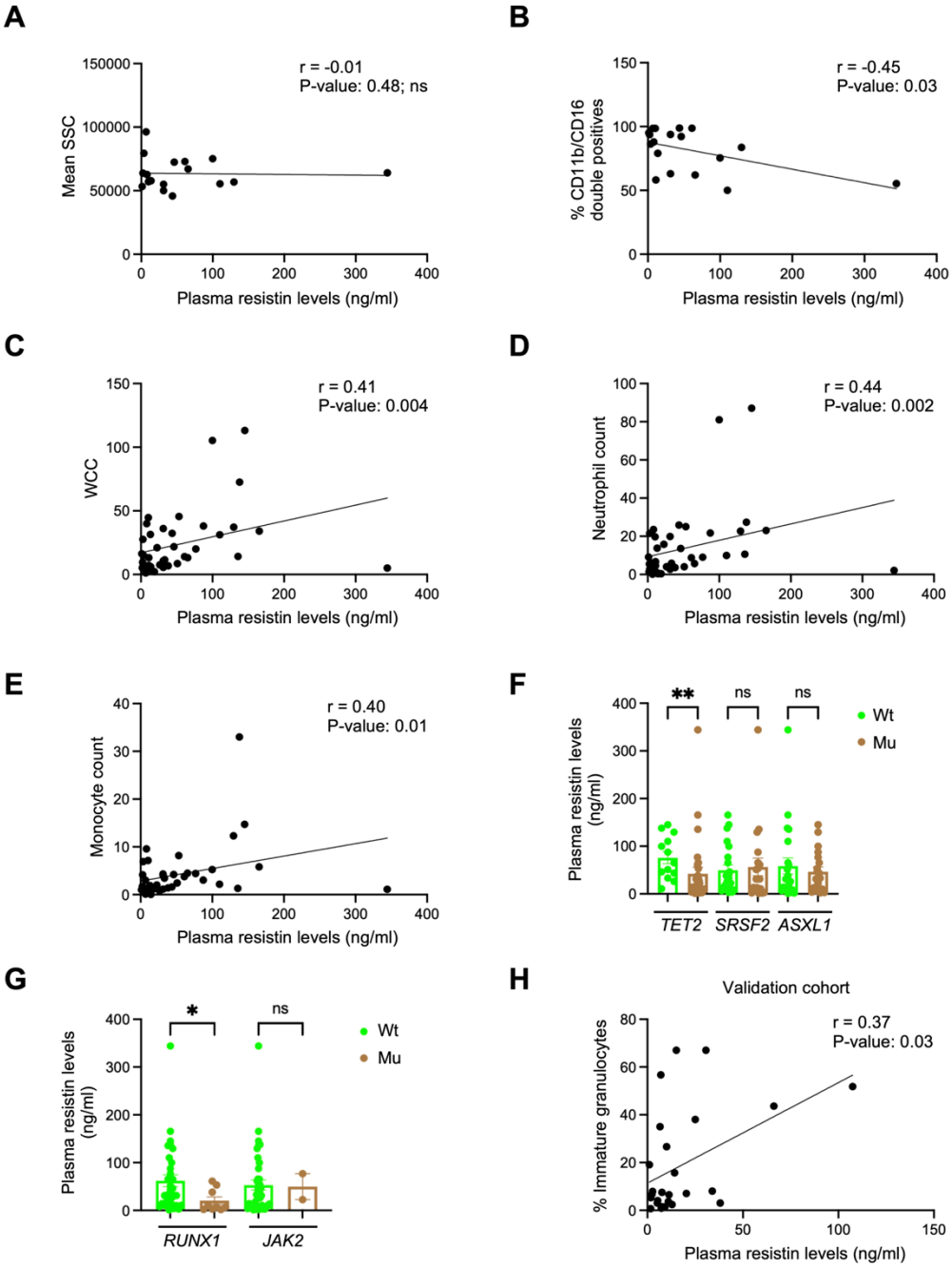
Supplemental Figure 2: (**A**) Bar graph showing average percentage of CD11b/CD16 double positive mature granulocytes in wild-type and mutant genotype of indicated genes observed in CMML patients, and controls. (**B**) A representative flow cytometry plot (left) displaying gating strategy used to sort low-density granulocytes (LDGs) and high-density granulocytes (HDGs). A representative flow cytometry plot (right) displaying the side scatter profile of LDGs and HDGs sorted from CMML patient granulocytes (n = 4). (**C**) Tables displaying the variant allele frequencies of indicated mutations in LDGs and HDGs sorted from 4 different CMML patient granulocytes. (**D**) Bar graph illustrating percentage of CD11b/CD16 double positive mature granulocytes between CMML disease subtypes dysplastic (MD-CMML, n = 9) and proliferative (MP-CMML, n = 24). (**E**) Kaplan-Meier AML-free survival plot of CMML patients stratified by the percentage of immature CD11b+/CD16- low (n = 15) and high (n = 20) granulocytes. (**F**) Spearman's correlation between percentage of immature granulocytes and neutrophil-to-monocyte ratio in peripheral blood of CMML patients (n = 34). Error bars = ± SEM; (**A** and **D**) Mann-Whitney test; ns, no significance; **, P<0.01.



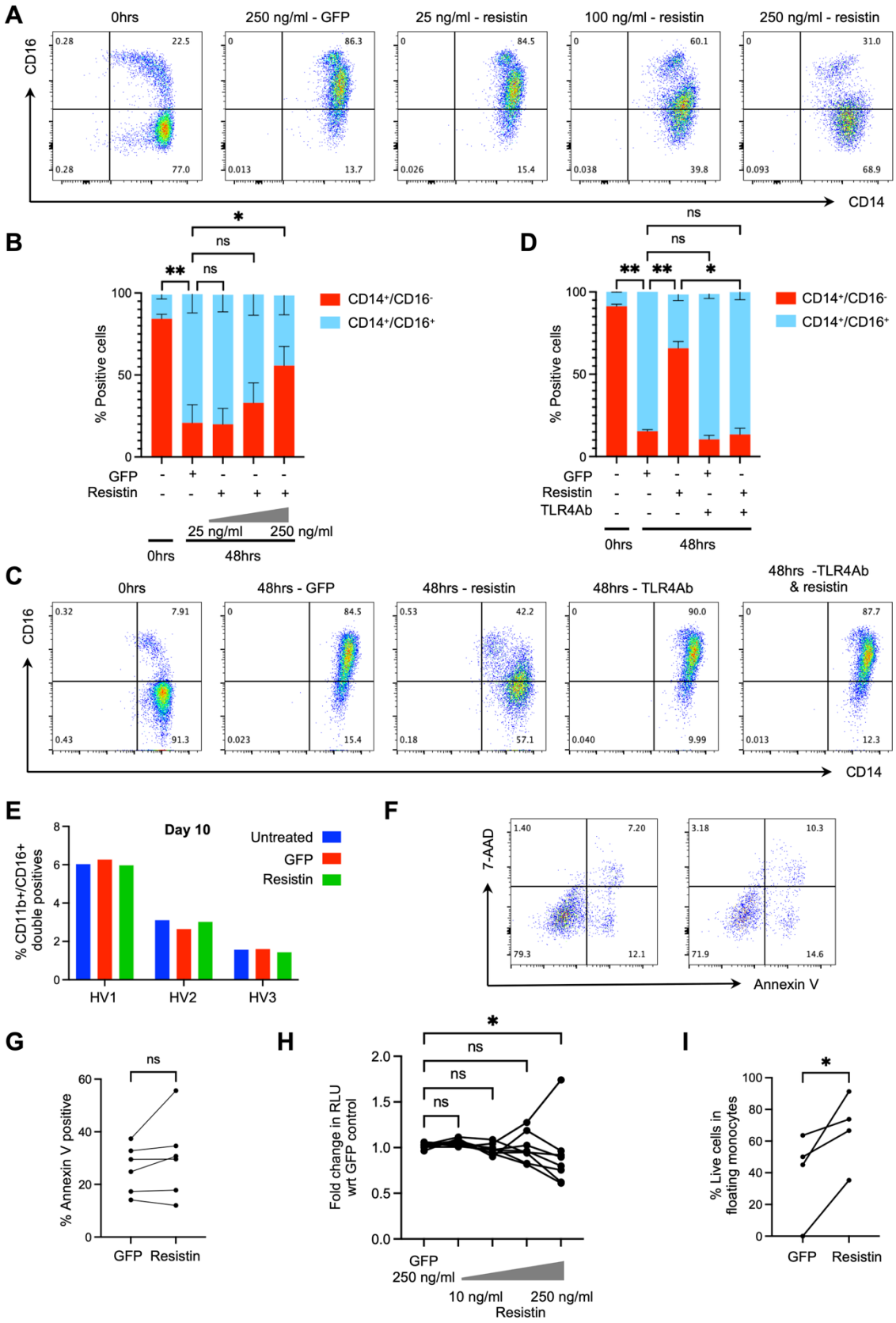
Supplemental Figure 3: (**A**) Gene ontology analysis of downregulated genes in CMML granulocytes as compared with controls. Top ten significant pathways are shown. (**B**) Mean centered expression analysis of indicated pro- or anti-apoptotic genes in old control and CMML granulocytes. (**C** and **E**) Relative expression levels of indicated genes as determined by q-RT-PCR in CMML granulocytes in comparison with granulocytes from age matched controls. (**D**) Normalized expression levels of selected downregulated genes in CMML granulocytes as compared with control young and old granulocytes. (**F**) GSEA plot showing relative enrichment of a gene set linked to CSF3/G-CSF signaling. (**G**) Mean centered expression analysis of indicated genes related to neutrophil activation in old control and CMML granulocytes. Error bars = ± SEM; (**C** and **E**) Welch's t test, except *DEFA4A* and *ELANE* plots where Mann-Whitney test was used due to failing normality test; (**D**) Wald test with Benjamini–Hochberg correction; *, P<0.05; **, P<0.01; ***, P<0.001; ****, P<0.0001.



Supplemental Figure 4: (**A**) Normalized expression levels of *RETN* in different normal hematopoietic cell types. Data plotted from Bloodspot (1). (**B**) Normalized expression levels of *RETN* at single cell level in different normal hematopoietic cell types (data reanalyzed from (2)). (**C**) Normalized expression levels of *RETN* in different stages of granulocyte development. PM: Promyelocyte, MM: Metamyelocyte, BN: Band Neutrophil SN: Segmented neutrophil, PMN: Polymorphic neutrophil. (**D**) UMAP based on highly variable genes expressed in PBMNCs of 4 CMML patients (data analyzed from (3)) colored by cluster type. Clusters annotated as different cell types is indicated. (**E**) UMAP plots overlaid with expression levels of indicated genes. (**F**) Normalized expression of *RETN* in different clusters annotated as mature granulocytes (C11), immature granulocytes (C5 and C8), T cells (C1 and C4) and NK cells (C0 and C6).

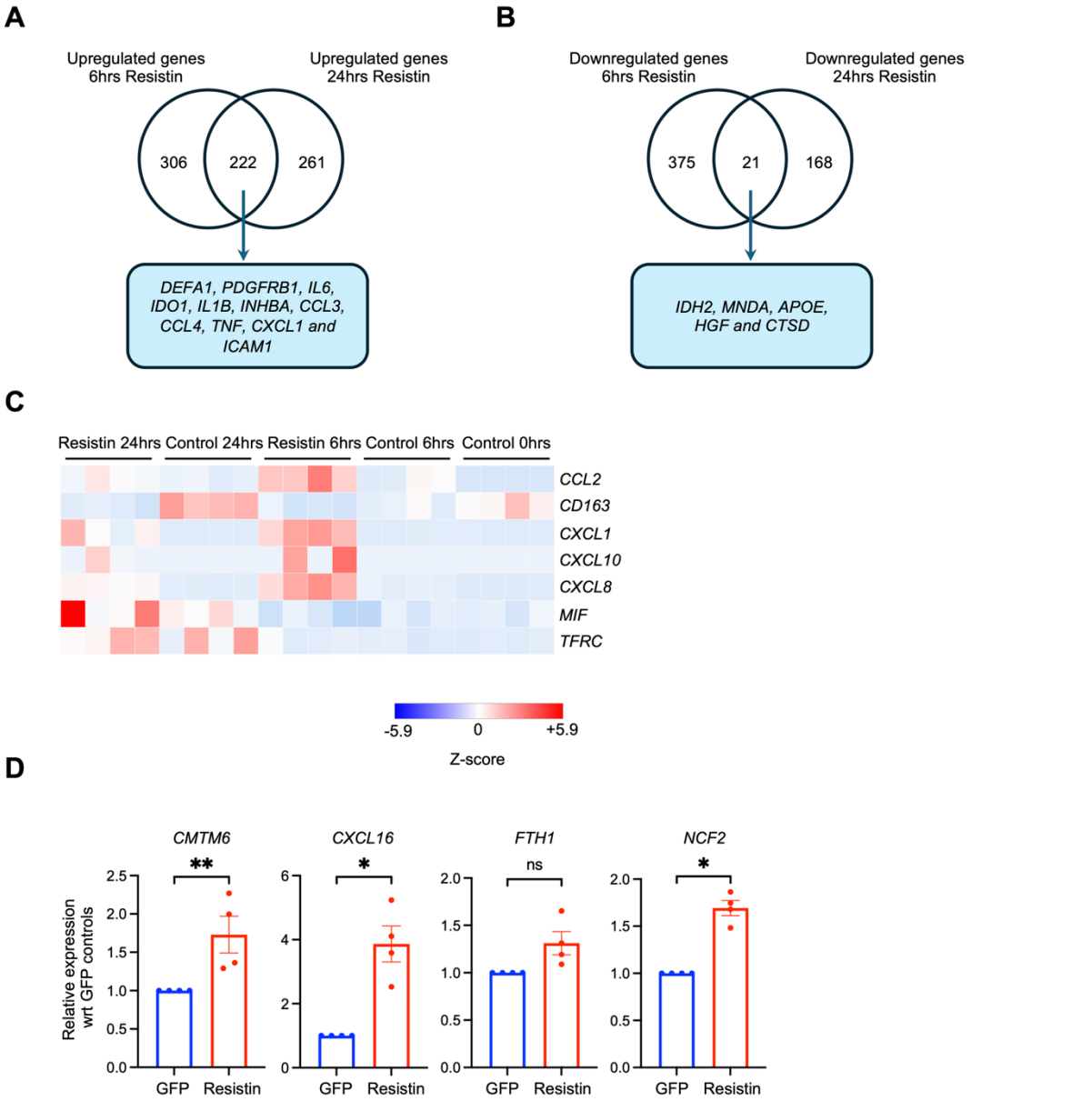


Supplemental Figure 5: (**A** and **B**) Spearman's correlation between plasma resistin levels with mean SSC (**A**) or fraction of CD11b/CD16 double positive cells (**B**) in CMML granulocytes. (**C**-**E**) Spearman's correlation between plasma resistin levels with mean whole cell count (**C**), neutrophil count (**D**) and monocyte count (**E**). (**F** and **G)** Bar graph showing average plasma resistin levels (ng/ml) in wild-type and mutant genotype of indicated mutated genes seen in CMML patients. (**H**) Spearman's correlation between plasma resistin levels with percentage of immature granulocytes identified in PBMNCs of a validation cohort. Error bars = ± SEM; (**F** and **G**) Kruskal-Wallis test; ns, no significance; *, P<0.05; **, P<0.01.

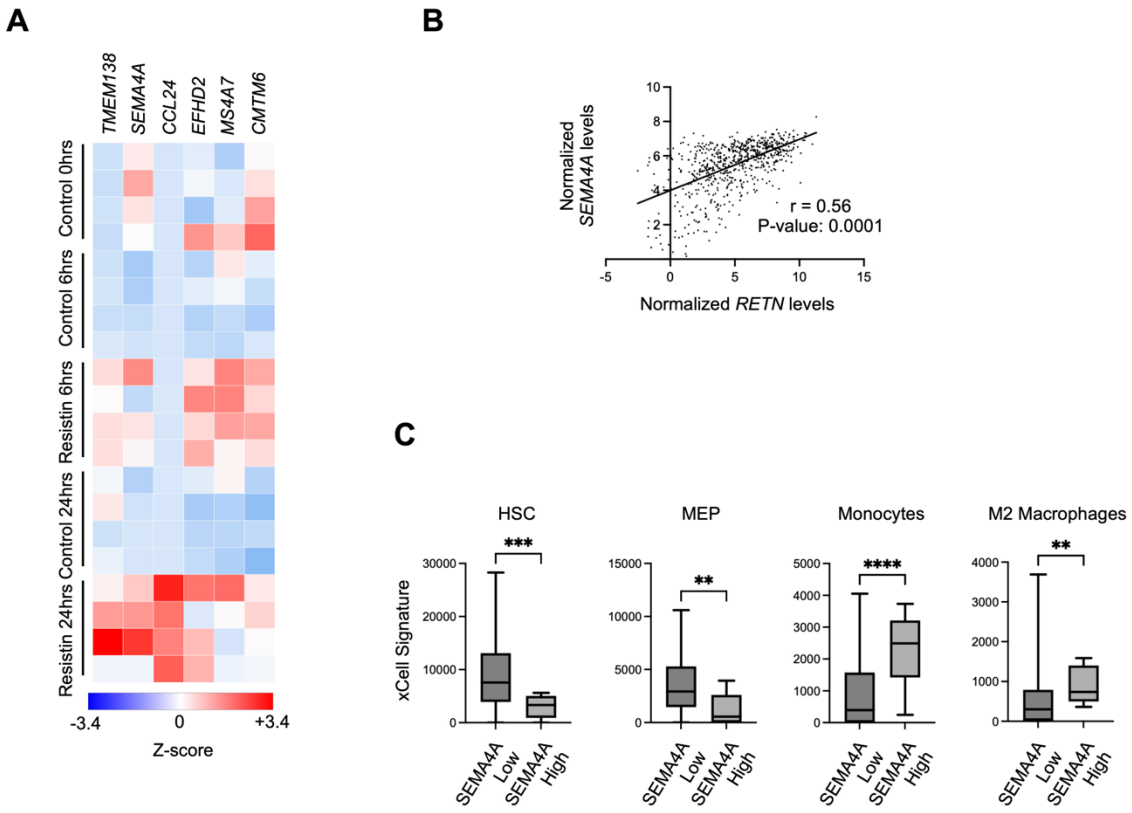


Supplemental Figure 6: (**A**) Representative flow cytometry plots showing the surface marker expression of CD14 and CD16 on freshly isolated healthy monocytes (0 hrs) and monocytes treated with increase in concentration of resistin or control GFP for 48 hrs (n = 5). (**B** and **D**) Bar charts showing average percentage of CD14+CD16- or CD14+CD16+ populations under indicated conditions. (**C**) Representative flow cytometry plots showing the surface marker expression of CD14 and CD16 on monocytes incubated with or without TLR4 neutralizing antibody (TLR4Ab) prior to exposure with

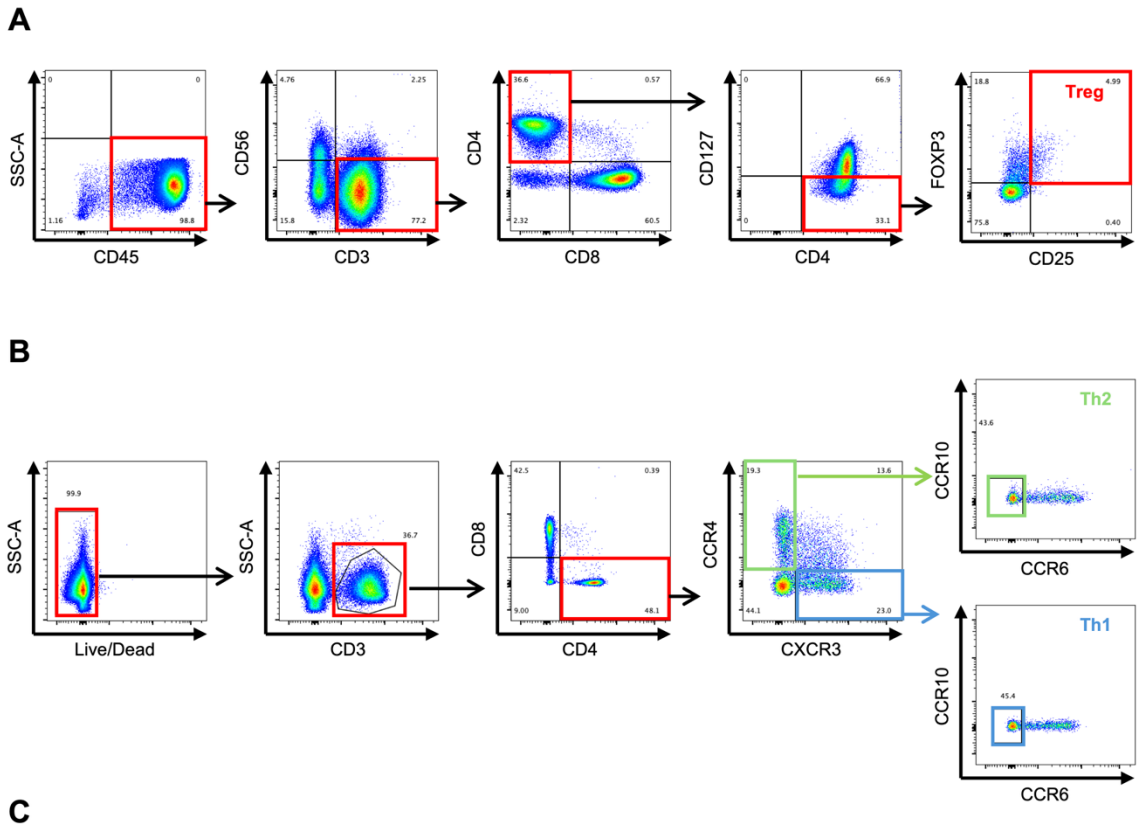
resistin or GFP control for 48 hrs (n = 4). (**E**) Percentage of mature granulocytes ($CD11b^{+}CD16^{+}$) observed on day 10 following differentiation of healthy CD34 positive HSPCs (n = 3; HV1-HV3) cultured in presence of recombinant resistin, recombinant GFP (control), or no treatment. (**F**) Representative flow cytometry plots displaying Annexin V/7AAD levels on CMML monocytes treated with GFP or resistin for 72 hrs. (**G**) Dot plot showing the percentage of Annexin V positive cells when CMML monocytes are treated with resistin in comparison with GFP control (n = 6). (**H**) Cell viability determined by CellTiter-Glo assay of CMML monocytes treated with either increase in concentration of resistin (10 ng/ml to 250 ng/ml) or control GFP (250 ng/ml) for 72 hrs (n = 8). Fold change in relative luminescence units (RLU) in CMML monocytes treated with resistin with respect to GFP control is shown. (**I**) Percentage of live undifferentiated monocytes in suspension cultures of monocyte differentiation, treated either with GFP control or resistin. N.B. 0 hrs data shown in **A** and **B** is the same data from Figures 4A and B, whilst 0 hrs in **C** and **D** is also shown in Figures 4C and D. Error bars = ± SEM; (**B** and **H**) Friedman test; (**D**) RM one-way ANOVA; (**G**) Wilcoxon test; (**I**) Paired t test; ns, no significance; *, $P<0.05$; **, $P<0.01$.

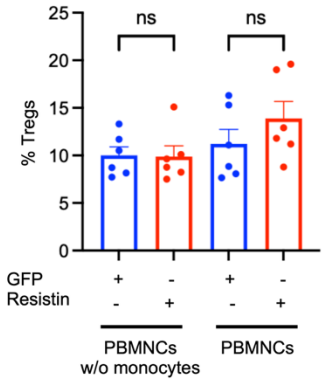


Supplemental Figure 7: (A) Venn diagram showing overlap of differentially expressed genes upregulated following 6 hrs and 24 hrs treatment with resistin in comparison with their respective time point GFP treated controls. **(B)** Venn diagram showing overlap of differentially expressed genes downregulated following 6 hrs and 24 hrs treatment with resistin in comparison with their respective GFP treated time point controls. **(C)** Mean centered expression analysis of indicated genes related to monocyte activation in different experimental conditions as indicated. **(D)** Relative expression levels of indicated genes as determined by q-RT-PCR in healthy monocytes treated with resistin for 24 hours in comparison with GFP treated cells. Error bars = ± SEM; Paired t test; ns, no significance; *, P<0.05; **, P<0.01.



Supplemental Figure 8: (**A**) Mean centered expression analysis of indicated genes commonly upregulated at 6 hrs and 24 hrs of resistin treatment, but not by LPS, in healthy monocytes as compared to GFP control. (**B**) Spearman's correlation between expression levels of *RETN* and *SEMA4A* in AML samples (4). (**C**) Comparisons of xCell signatures revealing distinct enrichment of specific hematopoietic cell signatures in *SEMA4A* high vs low CMML bone marrow nuclear cells (n = 11, High; n = 79, Low). HSC: Hematopoietic stem cells. MEP: Megakaryocyte erythroid progenitors. Error bars = ± SEM; (**C**) Mann-Whitney test; **, P<0.01; ***, P<0.001; ****, P<0.0001.





Supplemental Figure 9: (**A** and **B**) Representative flow cytometry plots displaying the gating strategy to analyze T-reg population (**A**) or Th2/Th1 cell ratio (**B**). (**C**) Percentage of Treg cells in ex vivo cultures of whole- or CD14 depleted-PBMNCs treated with either GFP or resistin for 9 days (n = 6). Error bars = ± SEM; RM one-way ANOVA; ns, no significance.

Supplemental methods:

Granulocyte characterization: Sorted granulocytes (1 x 10^5 cells) were stained with CD14-FITC (Invitrogen, 11-0149-42), CD16-APC-H7 (BD Biosciences, 560195), CD13-PE-Cy7 (BD Biosciences, 561599), CD11b-PE (Invitrogen, 12-0118-42) and CD66b-APC (Invitrogen, 17-0666-42) to profile purity and maturation status of granulocytes. Cells were analyzed on a BD LSR II flow cytometer. In total, we have analyzed granulocytes from twenty-one healthy volunteers and thirty-five CMML patients in this study. Flow data (from 12 controls and 12 *TET2* mutant CMML patients) from our previous study (5) was reanalyzed and used in this study.

PB smear analysis: A 3 μl drop of fresh PB from aged healthy or CMML patients was placed on a slide, smeared and left to air dry. Blood smears were fixed and stained in May-Grunwald's staining solution (Sigma-Aldrich; 1.01424) for 5 minutes, briefly rinsed with 1x Sorensen buffer pH 6.8 (Atom Scientific; RRPBS2-10) and further stained in 10% Giemsa stain (Sigma-Aldrich; 1.09204) for 20 minutes. Slides were rinsed with distilled water and left to air dry. Images were taken at 40x magnification on Invitrogen EVOS XL Core Imaging System.

Granulocyte and monocyte RNA extraction and sequencing: RNA was extracted from 5 x 10^5 granulocytes from fourteen healthy volunteers (seven young, seven old) and fourteen CMML donors using the RNeasy Micro Plus kit (QIAGEN, 74034), according to manufacturer's recommendations. $CD14^+$ monocytes from aged healthy volunteers were seeded at 5 x 10^5 cells/ml in 12-well plates with monocyte complete medium - RPMI media (Gibco, 21875) containing 10% HI FBS, 1% penicillin-streptomycin (Sigma-Aldrich, P0781), and 10 ng/ml M-CSF (Peprotech, 300-25) and treated with either 250 ng/ml GFP or resistin or 100 ng/ml LPS (Sigma-Aldrich L2630) for 6 or 24 hrs. Cells were then harvested, washed in PBS and RNA extracted using RNeasy Micro Plus kit. RNA was then sequenced 3' single end using the Novaseq SP instrument 1 x 100 cycles.

Phagocytosis assay: A total of 1 x 10^5 granulocytes from nine aged healthy and fifteen CMML donors were resuspended in HBSS (Gibco, 14025-092) containing 10 mM HEPES (Gibco, 15630-080) and 3% HI FBS and incubated at 37°C for 30 minutes with/without Zymosan A (S. cerevisiae) BioParticles, Alexa Fluor 488 conjugated, (ThermoFisher, Z23373) at MOI 10:1, according to manufacturer's protocol. Activity was stopped by adding ice-cold PBS, centrifuging 300 x g for 5 mins at 4°C and washing twice in ice-cold PBS. Bioparticle uptake was measured by flow cytometry on BD FACS Canto instrument.

NETosis assay: Freshly isolated granulocytes from seven aged healthy controls and seven CMML patients were seeded into a 24-well plate at a concentration of 1 x 10^6 cells/ml and left untreated or stimulated with 20 nM PMA and incubated at 37°C for 4 hours, following the NETosis assay kit protocol (Abcam, ab235979). Following stimulation and NET formation, cells and supernatant were aspirated, wells washed twice with NET assay buffer before addition of S7 Nuclease (15 U/ml) for 15 minutes at 37°C to disrupt NETs. Supernatants were then transferred to microtube tubes, with addition of EDTA to

inactivate Nuclease activity, and centrifuged at 300 x g for 5 minutes. Supernatants were transferred to fresh microtube tubes and stored at -20°C until ready to perform neutrophil elastase assay. Briefly, 100 µl of supernatant was added to 96-well plate in duplicate and equal volume of NET assay Neutrophil Elastase Substrate was added to each well, plate covered and incubated at 37°C for 1 hr. Absorbance was read at 405 nm and Elastase activity calculated for each sample by plotting a standard curve of concentration of known standards vs absorbance.

Monocyte isolation and resistin treatment: PB from aged healthy volunteers was diluted 1:1 with PBS and underwent density gradient separation by layering onto an equal volume of Ficoll-Paque Plus (Cytiva, 17144003) and centrifuged at 400 x g for 20 minutes at 20°C with no brake deceleration and acceleration set at 3 in Eppendorf 5810R centrifuge. The white layer containing mononuclear cells (MNCs) was collected and incubated for 3 minutes at RT in ACK-lysis buffer (Gibco, A1049201) for red blood cell removal. Cells were washed twice in PBS and counted. $CD14^+$ monocytes were isolated by magnetic activated cell sorting (MACS) using CD14 microbeads (Miltenyi, 130-050-201), following manufacturer's protocol. Isolated $CD14^+$ monocytes were seeded out at 1 x 10^5 cells/ml in 24 well plates in monocyte complete medium with GFP control (Abcam Ltd, ab84191) or resistin (Cambridge Bioscience, 230-00271-100) and incubated at 37°C, 5% CO_2 for 24- and 48-hrs. Following incubation, cells were harvested and stained with CD14-FITC and CD16-APC-H7 or SEMA4A-APC (BioLegend, 148405) and analyzed by flow cytometry on BD FACS Canto.

Macrophage differentiation: $CD14^+$ monocytes were isolated from four healthy volunteers and seeded out at 1 x 10^6 cells/ml in a 6 well plate in monocyte complete medium containing 25 ng/ml M-CSF and exposed to either 250 ng/ml GFP endotoxin control or recombinant resistin in duplicate. Cells were incubated for 6 days at 5% CO_2 and 37°C, with fresh complete medium containing treatment added on Day 3. On Day 6 cell confluency of attached cells was calculated using the AI Cell Confluency module (Labscope software) of a Zeiss Axiovert 5 digital microscope. Media was harvested and the number of viable suspended cells calculated using trypan blue and an Invitrogen Countess 3 Cell Counter.

Monocyte TLR4 treatment: $CD14^+$ monocytes from four aged healthy volunteers were seeded out at 2 x 10^5 cells/ml in 48 well plates with monocyte complete medium and pretreated for 1 hr with/without 10 µg/ml TLR4 neutralizing antibody (R&D systems, AF1478) at 37°C, 5% CO_2. After pretreatment, cells were treated with either GFP control or 250 ng/ml resistin and incubated for 24- and 48-hrs. Following incubation cells were stained with CD14-FITC and CD16-APC-H7 antibodies and analyzed by flow cytometry on BD FACS Canto.

Healthy $CD34^+$ differentiation to granulocytes: HSPCs were isolated from three cryopreserved G-CSF mobilized PB of healthy donors via first depletion of non-viable cells with dead cell removal kit (Miltenyi, 130-090-101), followed by CD34 isolation using microbeads (Miltenyi, 130-046-702), according to manufacturer's protocol. To increase $CD34^+$ purity, the isolated fraction of the first sort was passed through a second column and purity checked via flow cytometry. Culture and differentiation of

HSPCs was adapted from Webbers et al. (6). Briefly, $CD34^+$ isolated cells were seeded out at 0.5 x 10^6 cells/ml in StemSpan SFEM (STEMCELL Technologies, 09650) and 1% penicillin-streptomycin supplemented with 500 ng/ml hSCF (Peprotech, 300-07), 250 ng/ml hFlt-3L (Peprotech, 300-19), 10 ng/ml hIL-3 (Peprotech, 200-03), 10 ng/ml hGM-CSF (Peprotech, 300-03) and 30 ng/ml hG-CSF (Peprotech, 300-23) and incubated for 3 days at 37°C, 5% CO_2 for 3 days. On days 3, 7, 10 and 14 medium was completely changed and only hG-CSF was used in the medium with addition of either 250 ng/ml GFP or resistin. Upon day 10, cells were brought and maintained at a concentration of 1 x 10^6 cells/ml. Maturity of granulocytes was assessed by flow cytometry analysis for markers CD14-FITC, CD16-APC-H7, CD13-PE-Cy7, CD11b-PE, and CD66b-APC on day 10 and 14 using BD LSR II instrument.

PBMNC co-culture with resistin: PBMNCs with or without depletion of $CD14^+$ cells were seeded at 1 x 10^6 cells/ml in 6 well plates with T-cell complete medium - RPMI supplemented with 10% HI FBS, 1% penicillin-streptomycin, 25 ng/ml M-CSF, 20 IU/ml IL2 (Chiron), 10 ng/ml IL7 (Peprotech, 200-07), 1 mM sodium pyruvate (Corning, 25-000-CI), 1% MEM non-essential amino acid solution (Sigma-Aldrich, M7145), 25 mM HEPES and 50 nM 2-mercaptoethanol (Sigma-Aldrich, M6250) - and treated with GFP control or 250 ng/ml resistin for 9 days. Fresh T-cell complete medium containing GFP or resistin was added every 3 days. After the incubation period, cells were harvested, washed in SM buffer, counted and 1 x 10^6 cells were stained with Zombie UV viability stain, CD3-PerCP-CY5.5, CD4-BV605, CD8a-AF700; for Tregs the additional stains CD45-BV785, CD56-APC-Cy7, CD127-PE-CY7, CD25-APC and FOXP3-PE were used; for Th1/Th2 the additional stains CD183-BV421, CD194-PE-Cy7, CD196-PE and CCR10-APC were used. Cells were analyzed by flow cytometry on BD Fortessa and percentage of Treg or Th1 and Th2 cells was determined using FlowJo software.

Apoptosis assays: Six cryopreserved CMML PBMNCs were thawed and non-viable cells removed by dead cell removal kit, following manufacturer's protocol. $CD14^+$ cells were isolated by MACS and cultured in monocyte complete medium containing either GFP or 250 ng/ml resistin for 72 hrs at a density of 1 x 10^5 cells/ml in a 24-well plate. Following incubation, cells were harvested and washed once in PBS and then once in 1x annexin V binding buffer (AVBB) (Thermo Fisher Scientific, V13246). Cells were resuspended in AVBB containing Annexin V-APC (BioLegend, 640941) and incubated at RT for 15 minutes, protected from light. The cell suspension was then washed with AVBB and centrifuged at 400 x g for 5 minutes. Cells were resuspended in AVBB containing 7-AAD viability stain (BioLegend, 420404) and incubated at RT for 15 minutes. Following incubation, the cell suspension was topped up with AVBB and analyzed by flow cytometry on BD Fortessa.

CellTiter glo assays: Eight cryopreserved CMML PBMNCs were thawed and non-viable cells removed by dead cell removal kit. $CD14^+$ cells were isolated by MACS and cultured in monocyte complete medium containing either GFP or 10, 25, 100 or 250 ng/ml resistin for 72 hrs at a density of 1 x 10^4 cells/ml in a 96-well plate. Following incubation, equal volumes of CellTiter-Glo (Promega, G9243) was

added to the cell cultures, following manufacturer's recommendations. The relative luminescence was then measured using BMG Labtech FLUOstar Omega plate reader.

Transcriptome analysis (Granulocyte data): Sample libraries were prepared by 3' Quantseq (Lexogen) protocol and were sequenced using the Novaseq (Illumina) platform. Basecalls were converted to fastq files using bcl2fastq (Illumina). Fastq files were aligned to GRCh38 using Star aligner (version 2.5.1b; Ensembl85). BAM alignments were quantified in R (version 3.6.1) using featureCounts from the Rsubread library (version 2.0.1) and the Ensemble GTF annotation (Homo_sapiens.GRCh38.85.gtf). Differential expression (DE) was evaluated comparing the gene level integer read count data for between patient/sample groups using the DESeq2.v 1.26.0 Bioconductor package. DESeq2 DEG estimation involves multiple steps. In brief, it uses normalization factor to model read counts to account for sequencing depth. Then it estimates gene-wise dispersions and perform shrinkage analysis to generate more accurate estimates of dispersion to model the counts. Finally, it fits the negative binomial model and performs hypothesis testing using the Wald test.

Transcriptome analysis (Monocyte data): Quality of FASTQ files was evaluated using the FASTQC (v.0.12.1) and MULTIQC (v.1.15) software. MULTIQC adapter content check passed with no warnings, suggesting against need for adapter trimming. Reads were mapped to the reference GENCODE transcriptome (release v42; GRCh38.p13/hg38) using the STAR (v.2.5.1b) aligner with the parameter *–quantMode TranscriptomeSAM*. The resulting *Aligned.toTranscriptome.out bam* files from STAR were then used as impute for transcripts counts quantification via Salmon (v.1.10.2) using the alignment-based mode and the following parameters: *--libType A, --gcBias, --seqBias*. The following downstream analysis was then performed using R (v.4.3.3). Gene-level abundances (TPMs) and counts were estimated via using the package TxImport (v.1.30.0). Transcript-level counts contained within Salmon-produced *quant.sf* files were processed with the *tximport* function, setting parameter *countsFromAbundance ="no"* for subsequent DESeq2 (v.1.42.1) offset method and using a reference transcript to gene dictionary. This was generated from a txDb object obtained via GenomicFeatures (v.1.54.4) package using the function *makeTxDbFromGFF* on a GENCODEv42 gtf reference file.

Differentially expressed genes (DEGs) were computed using DESeq2 importing gene counts with the *DESeqDataSetFromTximport* function. Following library size estimation, genes with <5 counts across a minimum of 3 samples were removed. A minority (0.002%) of Ensembl genes mapping to the same gene symbol were also filtered to maintain only the most informative duplicate with the highest base mean expression. Following filtering, *DESeq2* function was run using *'local'* fit to model gene expression, since this resulted in the best fitting model with the least residuals. Finally, counts were normalized by condition (*design = ~Condition*) and transformed using the regularized log transformation (rlog), which accounts for gene dispersion and results in a log2 scaled count matrix. DEG analysis was performed implementing the independent hypothesis weighting (IHW) pvalue correction to increase

detection rate. Results were sorted by increasing p.adjusted value. Rlog counts were used for visualization purposes, including heatmap representations.

Gene set enrichment analysis (GSEA) (v.4.3.3) was used (7, 8). The normalized expression values were used as an input for this analysis. Gene set permutation as opposed to phenotype permutation was used, due to sample size, to calculate significance. 1000 permutations were used.

Single cell data analysis (healthy bone marrow): The differential expression of *RETN* per cell type was determined from samples of healthy bone marrow aspirates from (9) which were downloaded from NCBI's Sequence Read Archive: SRR22351039, SRR22351042, SRR22351043, and SRR22351045. Raw FASTQ files were downloaded using NCBI's 'fasterq-dump' program and renamed to fit the naming convention required for analysis with 10x Genomics Cell Ranger. The paired-end FASTQ files were processed with the 10x Genomics Cell Ranger v9.1.0, using the cellranger count command and the transcriptome reference of GRCh38 published by 10x Genomics and the '--create-bam' parameter set to 'true'. We used the resulting tables to create raw UMI counts tables for each of the four samples. Each sample was subsequently filtered and cleaned with scanpy v1.11.2 Click or tap here to enter text.using the following criteria: 1) remove cells if more than 10% of their UMIs mapped to mitochondrial genes, 2) remove cells in which 100 genes or less were expressed, 3) remove genes expressed in 3 cells or less, and 4) remove predicted doublet cells. Next, we annotated cells by cell type using the SingleR (10) package (v2.8.0) in R v4.4.4 with default parameters, and the scRNA-seq expression data of (11) as published in their GitHub repository (github.com/ andygxzeng/BoneMarrowMap?tab=readme-ov-file). Cells were annotated following the 'pruned labels' column of SingleR's results, which are the labels with the highest confidence, and cells without a pruned label were labelled as 'Ambiguous'. These annotations were incorporated into an AnnData object using the anndata python module. For determining RETN expression levels across all cells, all samples were merged into one using anndata's '.concat' module, and violin plots of RETN expression were done with a bespoke python script (github.com/carlosj-rr/misc-sequence-analysis/blob/master/violins_withscan.py). This script extracts the cell types in which RETN is expressed and then plots as violin plots the distribution of RETN expression per cell type across all samples.

Single cell data analysis (CMML PBMNCs): The expression of *RETN* at single cell level was determined from samples of PBMNCs from CMML patients (3). The data analysis was performed as described in the original study (3).

References:

1. Gislason MH, Demircan GS, Prachar M, Furtwangler B, Schwaller J, Schoof EM, et al. BloodSpot 3.0: a database of gene and protein expression data in normal and malignant haematopoiesis. *Nucleic Acids Res.* 2024;52(D1):D1138-D42.
2. Montalban-Bravo G, Ma F, Ganan-Gomez I, Kanagal-Shamanna R, Adema V, Wei Y, et al. *Blood*. Content Repository Only!; 2021:2588.
3. Deschamps P, Wacheux M, Gosseye A, Morabito M, Pages A, Lyne AM, et al. CXCL8 secreted by immature granulocytes inhibits WT hematopoiesis in chronic myelomonocytic leukemia. *J Clin Invest.* 2024;134(22).
4. Bottomly D, Long N, Schultz AR, Kurtz SE, Tognon CE, Johnson K, et al. Integrative analysis of drug response and clinical outcome in acute myeloid leukemia. *Cancer Cell.* 2022;40(8):850-64 e9.
5. Huerga Encabo H, Aramburu IV, Garcia-Albornoz M, Piganeau M, Wood H, Song A, et al. Loss of TET2 in human hematopoietic stem cells alters the development and function of neutrophils. *Cell Stem Cell.* 2023;30(6):781-99 e9.
6. Webbers SDS, Gankema AAF, van Oosterom F, Rojas-Rodriguez F, Koops DS, Klaus AK, et al. Characterization of human CD34(+) HSPC-derived neutrophils with limited myeloid-derived immunosuppressive cell activity. *iScience.* 2025;28(9):113404.
7. Mootha VK, Lindgren CM, Eriksson KF, Subramanian A, Sihag S, Lehar J, et al. *Nature Genetics*. 2003:267-73.
8. Subramanian A, Tamayo P, Mootha VK, Mukherjee S, Ebert BL, Gillette MA, et al. *Proceedings of the National Academy of Sciences of the United States of America*. National Academy of Sciences; 2005:15545-50.
9. Montalban-Bravo G, Thongon N, Rodriguez-Sevilla JJ, Ma F, Ganan-Gomez I, Yang H, et al. Targeting MCL1-driven anti-apoptotic pathways overcomes blast progression after hypomethylating agent failure in chronic myelomonocytic leukemia. *Cell Rep Med.* 2024;5(6):101585.
10. Aran D, Looney AP, Liu L, Wu E, Fong V, Hsu A, et al. Reference-based analysis of lung single-cell sequencing reveals a transitional profibrotic macrophage. *Nat Immunol.* 2019;20(2):163-72.

11. Zeng AGX, Iacobucci I, Shah S, Mitchell A, Wong G, Bansal S, et al. Single-cell Transcriptional Atlas of Human Hematopoiesis Reveals Genetic and Hierarchy-Based Determinants of Aberrant AML Differentiation. *Blood Cancer Discov.* 2025;6(4):307-24.